Chemical Science

EDGE ARTICLE

View Article Online
View Journal | View Issue

Cite this: *Chem. Sci.*, 2019, **10**, 1634

All publication charges for this article have been paid for by the Royal Society of Chemistry

A catalytic antioxidant for limiting amyloid-beta peptide aggregation and reactive oxygen species generation†

Luiza M. F. Gomes,[a] Atif Mahammed,[b] Kathleen E. Prosser,[a] Jason R. Smith,[a] Michael A. Silverman,[c] Charles J. Walsby,[a] Zeev Gross*[b] and Tim Storr*[a]

Received 19th October 2018
Accepted 27th November 2018

DOI: 10.1039/c8sc04660c

rsc.li/chemical-science

Alzheimer's disease (AD) is a multifaceted disease that is characterized by increased oxidative stress, metal-ion dysregulation, and the formation of intracellular neurofibrillary tangles and extracellular amyloid-β (Aβ) aggregates. In this work we report the large affinity binding of the iron(III) 2,17-bis-sulfonato-5,10,15-tris(pentafluorophenyl)corrole complex **FeL1** to the Aβ peptide ($K_d \sim 10^{-7}$) and the ability of the bound **FeL1** to act as a catalytic antioxidant in both the presence and absence of Cu(II) ions. Specific findings are that: (a) an Aβ histidine residue binds axially to **FeL1**; (b) that the resulting adduct is an efficient catalase; (c) this interaction restricts the formation of high molecular weight peptide aggregates. UV-Vis and electron paramagnetic resonance (EPR) studies show that although the binding of **FeL1** does not influence the Aβ–Cu(II) interaction ($K_d \sim 10^{-10}$), bound **FeL1** still acts as an antioxidant thereby significantly limiting reactive oxygen species (ROS) generation from Aβ-Cu. Overall, **FeL1** is shown to bind to the Aβ peptide, and modulate peptide aggregation. In addition, **FeL1** forms a ternary species with Aβ–Cu(II) and impedes ROS generation, thus showing the promise of discrete metal complexes to limit the toxicity pathways of the Aβ peptide.

Introduction

Alzheimer's disease (AD) is the most common form of dementia, representing between 50–75% of all cases.[1] In 2017, an estimated 50 million people worldwide suffered from dementia, and this number is projected to grow sharply due to increased life expectancy.[2] The lack of effective treatment strategies for AD, coupled with increased incidence, has stimulated extensive research efforts in this important field.[3]

Clinical diagnosis of AD is currently based on progressive loss of memory and impairment in cognition,[4] with final diagnosis requiring post-mortem examination of the brain to determine the severity of two neuropathological hallmarks; amyloid-β (Aβ) plaques and neurofibrillary tangles (NFTs). It is still unclear whether Aβ-plaques, NFTs, or both, are a cause or an effect of the neurodegeneration in AD.[5] NFTs are intracellular aggregates of oxidatively-modified and hyper-phosphorylated microtubule-associated protein tau,[6] while Aβ plaques are extracellular and contain the Aβ peptide as the major constituent. The Aβ peptide is a product of the amyloid precursor protein (APP), and a series of cleavage events by α-, β-, γ-secretases,[7] afford the Aβ peptide as predominantly $Aβ_{1–40}$ or $Aβ_{1–42}$ (a 40- or 42-residue peptide).[8] In addition, truncation at the N-terminus results in $Aβ_{3(p)–n}$, $Aβ_{4–n}$, and $Aβ_{11(p)–n}$ (where p refers to pyroglutamate) peptides that are also significant components of amyloid deposits.[9] Aβ can be found in three general forms in the brain: membrane associated, aggregated, and soluble. Most of Aβ is membrane-associated in healthy individuals, but in individuals with AD the aggregated and soluble fractions increase considerably.[8,10]

Early neuronal and pathological changes show indications of oxidative damage, indicating oxidative stress is involved in AD.[11] The cause of oxidative stress in AD has been attributed to a number of factors, including impaired cellular energy metabolism and/or Fenton-type processes involving redox-active metal-ions (Fe, Cu), and metal-containing aggregates.[12] Metal-ions, such as Zn, Cu and Fe, are essential for healthy organisms and brain function, and are tightly regulated under normal circumstances.[13] However, a change in metal-ion homeostasis in the brain has been associated with protein aggregation, and the generation of reactive oxygen species (ROS) in neurodegenerative diseases such as AD.[14] Metal-ions are present in increased concentrations in Aβ plaques in comparison to normal brain tissue, with concentrations of *ca.* 0.4 mM for Cu, 1 mM for Zn, and 0.9 mM for Fe.[13a,13b,15] Metal-

[a]*Department of Chemistry, Simon Fraser University, V5A-1S6, Burnaby, BC, Canada. E-mail: tim_storr@sfu.ca*

[b]*Schulich Faculty of Chemistry, Technion-Israel Institute of Technology, Haifa, 32000, Israel. E-mail: chr10zg@technion.ac.il*

[c]*Department of Biological Sciences, Simon Fraser University, V5A-1S6, Burnaby, BC, Canada*

† Electronic supplementary information (ESI) available. See DOI: 10.1039/c8sc04660c

ion binding can modify the aggregation pattern of Aβ, disrupt normal metalloenzyme activity, and facilitate the production of ROS.[10b,14a,14c,16] Recent studies have shown that the Aβ–Cu(II) complex exhibits detrimental catalytic ROS generation, particularly so in the presence of cholesterol and vitamin C, and is able to reduce O_2 generating the superoxide anion ($O_2^{\cdot -}$), hydrogen peroxide (H_2O_2), and hydroxyl radical ($\cdot OH$).[17]

As a result of the possible role of metal-ion dyshomeostasis in AD, the development of multifunctional metal binding molecules as therapeutics has been actively explored.[18] We, and others, have developed metal-binding agents with additional properties such as radical scavenging, peptide binding and aggregation inhibition, and acetylcholine esterase (AChE) activity.[19] In addition, a number of groups have explored the use of discrete metal complexes for the diagnosis and treatment of AD.[20] In terms of therapeutics, Pt,[21] Ru,[22] Ir,[23] Co,[10b,24] Re,[25] Rh,[26] Mn,[27] and V[28] complexes have been investigated for their ability to modify the aggregation of the Aβ peptide, and certain compounds have shown promising results in disease models. For example, an orally-available Pt(IV) complex (Scheme 1) was shown to cross the blood–brain barrier (BBB), reduce plaque burden, and reduce Aβ peptide levels in a APP/Ps1 mouse model.[29] Therefore, a metal complex that can bind to the Aβ peptide, modulate aggregation, and reduce ROS production is a promising therapeutic for AD.

Corrole ligands are known to bind to metal ions, such as Al, Cu, Fe, Ga, and Au, and the corresponding metal complexes display outstandingly high hydrolytic stability.[30] The iron(III) complex (**FeL1**, Scheme 1) displays excellent catalase activity,[31] superoxide dismutase (SOD) activity,[30a] and catalytic activity for the decomposition of peroxynitrite (PN, $ONOO^-$).[30d,32] Additionally, **FeL1** binds to and protects the cholesterol-carrying lipoproteins from oxidative stress; and oral administration of **FeL1** to a mouse model of atherosclerosis leads to a decrease in atherosclerotic lesions.[30c,33] We were thus interested to investigate the interaction of **FeL1** with the Aβ peptide, and how this would modulate peptide aggregation and ROS generation. Strong inspiration came from reports by Dey *et al.*, who have shown that heme binds to the Aβ peptide, that one of the three histidine residues (His[6]) of Aβ is ligated to the heme's iron, and that the heme-Aβ adduct induces ROS formation.[17a,34] Furthermore, a study that focused on the uptake of iron complexes by macrophages, which are a major source of ROS, revealed that heme is cytotoxic while **FeL1** is cytoprotective.[35] Additionally, **FeL1** was reported to have low cytotoxic activity while maintaining cell cycle distribution similar to untreated cancer cells.[36]

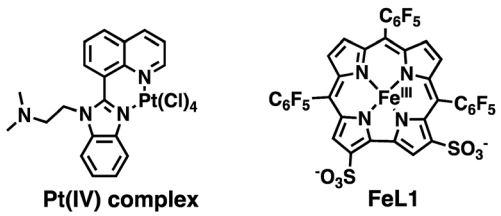

Scheme 1 Structures of Pt(IV) complex, and Fe(III) corrole (**FeL1**) complex.

We report the interaction of **FeL1** with the Aβ peptide, how it affects peptide aggregation, and the radical scavenging ability of the **FeL1**–Aβ adduct, in both the presence and absence of Cu(II) ions.

Results and discussion

Binding of Aβ His residues to FeL1

The Fe(III) complex of the amphipolar 2,17-bis-sulfonato-5,10,15-tris(pentafluorophenyl)corrole (**FeL1**) has very strong affinity to human serum albumin (HSA) and lipoproteins, which is in part due to binding of histidine (His) residues to the metal ion.[30c,37] The His ligation causes a shift in the Soret band of **FeL1** from 390 to 410 nm, as well as the formation of a new band at 620 nm, and the intensity of the latter band is associated with the binding of either one or two axial His residues.[30c,31,37] There are three Aβ His residues (His[6], His[13], and His[14]) and they play an important role in metal-ion binding (Scheme 2), with dissociation constants (K_d) of $\sim 10^{-10}$ M for Cu(II) and $\sim 10^{-5}$ M for Zn(II).[10b,14a,38] In addition, Aβ His residues have been reported to bind to discrete metal complexes such as heme,[34a] Ru complexes,[22a,23a,39] and Co complexes.[10b,24] In addition to His binding, residues Asp[1], Tyr[10], and Glu[11] play a role in the coordination of Aβ to Cu(II) and Zn(II).[40]

Prior to investigating the interaction(s) of **FeL1** with the Aβ peptide by UV-Vis spectroscopy, its binding to 1-methylimidazole (1-MeIm) was examined as to determine the spectral features and binding affinity associated with exogenous imidazole as the axial ligand. Gradual addition of up to 150 equiv. of 1-MeIm led to a shift in the near UV (Soret) band, a decrease in the band at 533 nm, and the formation of a new band at 620 nm (Fig. 1). The spectral changes matched those for histidine binding (Fig. S1†),[30c] however in both cases a large excess of ligand is required (150 and 700 equiv. respectively) to observe spectral endpoints. A variable pH UV-Vis titration (Fig. S2†), at a concentration ratio of 1 : 2 **FeL1** : 1-MeIm, together with subsequent data fitting using Hypspec and HySS,[41,45] provides binding constants of log M(1-MeIm) = 5.81 ± 0.01 (where M = **FeL1**) and a much smaller log M(1-MeIm)$_2$ = 2.57 ± 0.02. Our results are in accord with the higher stability of 5-coordinate mono-axial ligated Fe(III) corroles in comparison to 6-coordinate bis-axial ligated Fe(III) corroles,[42] which is opposite to that

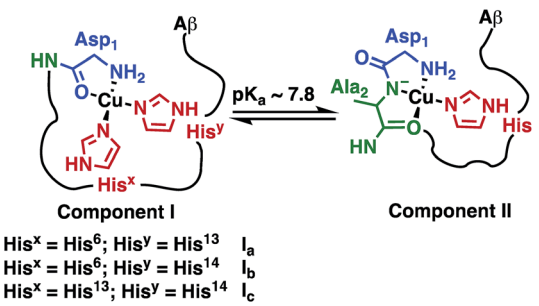

Scheme 2 Representation of Component I (I_a, I_b, I_c) and Component II, the two major pH-dependent Aβ–Cu(II) binding modes (modified from Borghesani *et al.*, 2018).[9c]

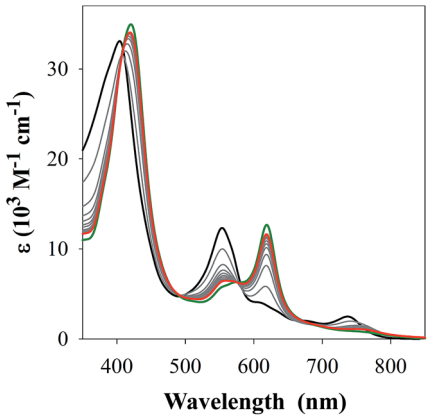

Fig. 1 UV-Vis spectra of 1-MeIm additions to **FeL1** (30 μM, black) in PBS buffer (0.01 M, pH 7.4). Grey lines represent additions of 5 equiv. of 1-MeIm up to 50 equiv. (red) with a maximum of absorption at 620 nm for 150 equiv. shown in green.

reported for Fe(III) porphyrins.[43] The main reason for this difference is that upon bis-axial ligation Fe(III) porphyrins gain more crystal field stabilization energy (CFSE) as they transform from high spin (HS) to low spin (LS), while Fe(III) corroles only transform from intermediate spin (IS) to LS.[42b,42c]

The studies with 1-MeIm provided critical information for examining the interaction of **FeL1** with the full length $A\beta_{1-42}$ and two truncated peptides: $A\beta_{1-16}$ that contains the metal binding N-terminus (His^6, His^{13}, His^{14}), and $A\beta_{17-40}$ with the hydrophobic portion of the peptide lacking any His. Addition of $A\beta_{17-40}$ to **FeL1** did not induce any significant spectral changes, while even a single equivalent of either $A\beta_{1-42}$ or $A\beta_{1-16}$ led to a red shift and intensity-increase of the Soret band, accompanied by the appearance of a $\lambda_{max} = 620$ nm band (Fig. 2). While this experiment clearly proves the importance of His–Fe binding, the comparison of Fig. 2 and 1 exposes major differences. Importantly, the binding of the protein-provided histidine must be much stronger than that of 1-MeIm as full spectra changes are achieved with 1 *vs.* >100 equivalents, respectively.

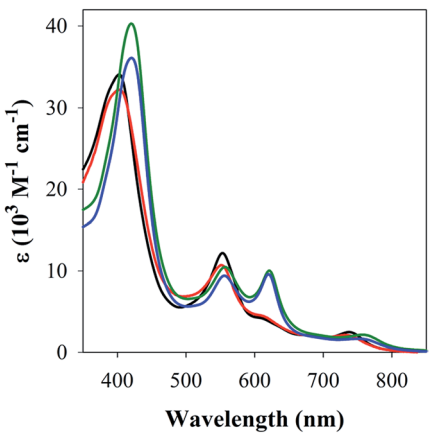

Fig. 2 UV-Vis spectra of **FeL1** (30 μM, black) in the presence of 1 equiv. of $A\beta_{17-40}$ (red), $A\beta_{1-16}$ (green) and $A\beta_{1-42}$ (blue) in PBS buffer (0.01 M, pH 7.4).

In the former case, the observed spectral changes occur immediately upon mixing, with no further spectral changes apparent after monitoring for 1 h, and addition of excess $A\beta_{1-16}$ (up to 16 equivalents, Fig. S3†) did not induce further spectral changes. The last result is also highly relevant to the other spectral difference: while the 533 nm band disappears in the presence of a large excess of 1-MeIm (Fig. 1), the bands at 533 and 620 nm remain of essentially equal intensity starting from a 1 : 1 (Fig. 2) to a 1 : 16 (Fig. S3†) ratio of **FeL1** : $A\beta_{1-16}$. Taken together, the results show that **FeL1** and Aβ form a 1 : 1 adduct that relies on only one of the His residues in Aβ. The other two His residues are either too far away to approach the metal center and/or are unable to bind due to steric interference. Previous reports agree with our findings in that axial ligand binding to Fe(III) corroles shows that the 5-coordinate species is stabilized in comparison to the 6-coordinate bis-axial ligated species.[42a,42b,44]

The stability of the 1 : 1 **FeL1** : $A\beta_{1-16}$ adduct was determined *via* a variable pH titration (Fig. 3), which together with subsequent data fitting using Hypspec and HySS,[41,45] provided binding constants of $\log M(A\beta_{1-16}) = 11.90 \pm 0.01$, and

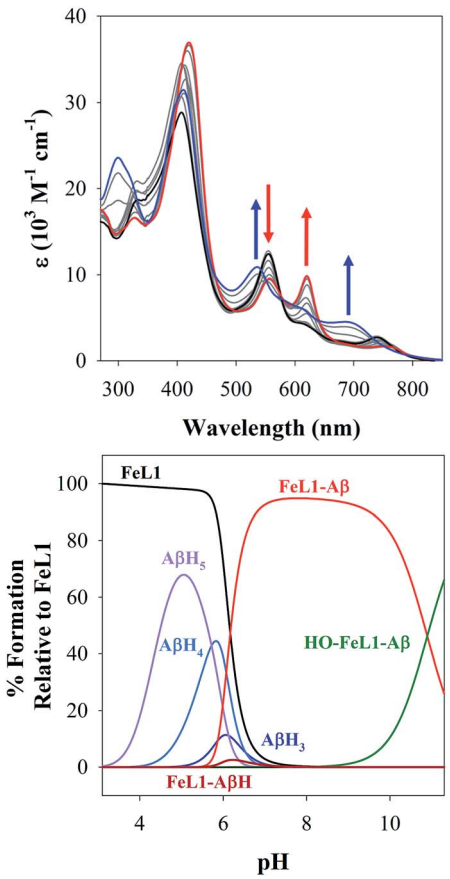

Fig. 3 (Top) variable pH UV-Vis titration of **FeL1** (30 μM) and $A\beta_{1-16}$ (30 μM) from pH 3.1 (black) to pH 11.5 (blue). The red spectrum represents the maximum absorbance for the **FeL1**–Aβ complex at pH 8.2. (Bottom) using HypSpec and HySS,[41] the variable pH data were fitted to a model including **FeL1**–Aβ, **FeL1**–Aβ(H), and a HO-**FeL1**–Aβ component at high pH. At pH 7.4 the majority of **FeL1** is bound to $A\beta_{1-16}$ (>99%).

log M($A\beta_{1-16}$)(H) = 4.90 ± 0.02 (where M = **FeL1**, and (H) indicates a mono-protonated peptide species). This experiment demonstrates the much higher affinity of **FeL1** for the Aβ peptide in comparison to 1-MeIm (see below). At higher pH values (>9.5) a metal hydrolysis species is evident (modelled as log M($A\beta_{1-16}$)(OH), presumably due to deprotonation of a bound H_2O ligand). As indicated from the speciation diagram (Fig. 3), the interaction of **FeL1** with the Aβ peptide coincides with His deprotonation (reported pK_a values of 5.72, 6.5, and 6.95).[46] Further analysis of the speciation diagram of **FeL1** with $A\beta_{1-16}$ provides the binding affinity at physiological pH. The concentration of free **FeL1** present in solution at a given pH, referred to as pM (p(**FeL1**) = $-\log[(\mathbf{FeL1})_{unchelated}]$), is a direct estimate of metal–ligand affinity when all species in solution are considered.[47] The calculated value for p(**FeL1**) is 6.6 ([**FeL1**] = [$A\beta_{1-16}$] = 30 μM), which affords a K_d value of $\sim 10^{-7}$ M.[18a,48] This value shows that the affinity of Aβ for **FeL1** is lower than for Cu(II) but larger than for Zn(II).

To gain more insight into the binding event, both ^{1}H NMR and ESI-MS studies were performed. The MS spectrum of a 1 : 1 **FeL1** : $A\beta_{1-16}$ adduct showed multiple *m*/*z* peaks consistent with **FeL1** binding to $A\beta_{1-16}$, with the most intense adduct peak corresponding to [**FeL1**–$A\beta_{1-16}$]$^{2+}$ (Fig. S5†). **FeL1** has been reported to bind to human serum albumin (HSA),[31] and in addition the Aβ peptide shows a specific interaction with HSA.[49] Based on these reports we investigated the binding of **FeL1** to Aβ in the presence of HSA, and under these conditions observed the [**FeL1**–$A\beta_{1-16}$]$^{2+}$ adduct (Fig. S6†). The ^{1}H NMR of $A\beta_{1-16}$ was recorded in the presence of 0.10 and 0.25 equivalents of the paramagnetic **FeL1**.[10b,50] Initially, the signals from the three histidines and the tyrosine were quite sharp and well resolved (Fig. 4, bottom trace). Addition of **FeL1** induced broadening of all signals attributed to the histidines (7.95, 7.05, 7.00 ppm), while those of Tyr^{10} (7.10 and 6.82 ppm) were not affected (Fig. 4, mid and top traces). Overall, the data are consistent with binding of an Aβ His residue to **FeL1**, and there is likely no preference for any of the available peptide His residues (His^6, His^{13}, His^{14}).

FeL1 binding to Aβ in the presence of Cu(II)

UV-Vis analysis. The affinity between Cu(II) and Aβ is very large (K_d of $\sim 10^{-10}$ M) and the inner coordination sphere of Cu(II) in the adduct is usually composed of the N-terminal amine, one carbonyl group and two histidines (Scheme 2, Component I, major species at pH = 7.4).[10b,14a,38a,51] Although the affinity of **FeL1** to Aβ was found to be quite large ($K_d \sim 10^{-7}$ M) it is still 3 orders of magnitude lower than that of Cu(II), and thus is not expected to compete for the Cu(II) binding site. Considering, however, that the Aβ–Cu(II) adduct still has one His residue not involved in Cu binding, concurrent binding of Cu(II) and **FeL1** to Aβ is possible and of large potential interest. This aspect was addressed by combining **FeL1** with a preformed Aβ–Cu(II) complex and also *vice versa*, by adding Cu(II) to a **FeL1**/peptide mixture. Identical results were obtained in both cases (Fig. 5 and S4†) and the corresponding UV-Vis spectra clearly revealed the earlier outlined spectral features associated with axial His binding. This shows that **FeL1** binds to the peptide even in the presence of Cu(II) and also provides another independent indication that the inner coordination sphere of **FeL1** has only one axial histidine ligand. The formation of the ternary adduct (1 : 1 : 1 **FeL1** : $A\beta_{1-16}$: Cu adduct) was further confirmed by ESI-MS, with *m*/*z* peaks corresponding to [**FeL1**–Aβ–Cu(II)]$^{2+}$ and sodium adducts (Fig. S5†).

EPR characterization. In order to better understand the binding of both Cu(II) and **FeL1** to the Aβ peptide, we analyzed the electron paramagnetic resonance (EPR) spectra of $A\beta_{1-16}$–Cu(II), **FeL1**–$A\beta_{1-16}$, and finally **FeL1**–$A\beta_{1-16}$–Cu(II). The EPR data for $A\beta_{1-16}$–Cu(II) are in agreement with previous reports;[12b,50,52] and simulation of the EPR spectra indicate the existence of both Component I and Component II therein (Scheme 2 and Fig. S7†). The simulation parameters are detailed in Table 1, and an approximate intensity ratio of 0.6 : 0.4 for Component I : Component II at pH 7.4 is in agreement with the measured pK_a value of 7.8 ± 0.5 (Scheme 2) *via* the Henderson–Hasselbalch equation.[12b,50]

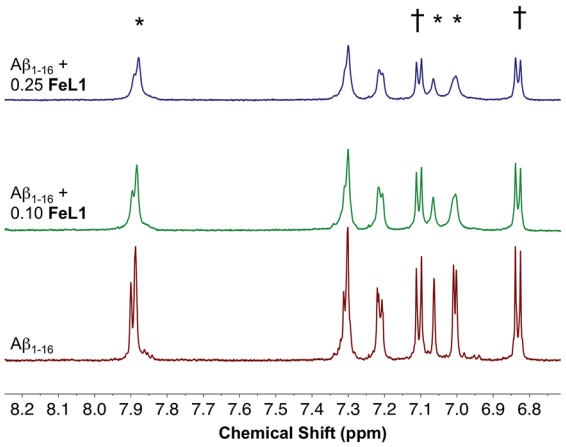

Fig. 4 Changes in the ^{1}H NMR spectra of $A\beta_{1-16}$ in the presence of **FeL1**. Shown are spectra obtained at 210 μM $A\beta_{1-16}$, in PBS buffer prepared in D_2O pH 7.4 at 25 °C (red), with addition of 0.10 (green) and 0.25 equivalents (blue) of **FeL1**. *His^6, His^{13}, and His^{14}. †Tyr^{10}.

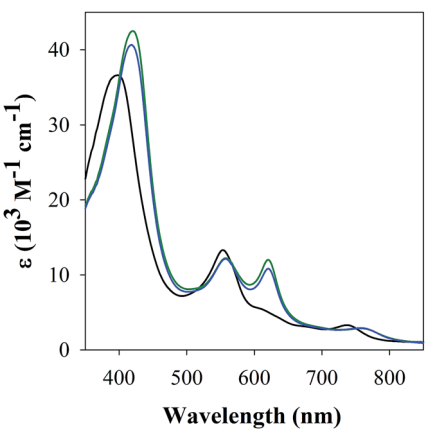

Fig. 5 UV-Vis spectra of binding of **FeL1** (30 μM, black) in PBS buffer (0.01 M, pH 7.4) to 1 equiv. of $A\beta_{1-16}$ with (blue) or without (green) Cu(II) (0.9 equiv.).

Table 1 X-band EPR simulation parameters[a]

	Aβ–Cu(II) – Component I				Aβ–Cu(II) – Component II				**FeL1** ($S = 3/2$)		Fe bound ($S = 1/2$)		
	$g_\parallel$	$g_\perp$	$A_\parallel^{Cu}$	χ^b	$g_\parallel$	$g_\perp$	$A_\parallel^{Cu}$	χ^b	$g_\parallel$	$g_\perp$	g_1	g_2	g_3
Aβ–Cu(II)	2.26	2.05	186	0.6	2.22	2.05	170	0.4	—	—	—	—	—
FeL1	—	—	—	—	—	—	—	—	2.0	3.9	—	—	—
FeL1 MeIm	—	—	—	—	—	—	—	—	2.0	3.9	2.70	2.2	1.8
FeL1–Aβ	—	—	—	—	—	—	—	—	2.0	3.9	2.75	2.2	1.7
FeL1–Aβ–Cu(II)	2.26	2.05	186	0.7	2.22	2.05	170	0.3	2.0	3.9	2.75	2.2	1.7

[a] See experimental section for details. [b] Component relative abundance.

FeL1 in buffer displays a weak intermediate-spin Fe(III) signal at $g_\perp = 3.9$ and $g_\parallel = 2.0$,[42b,53] whereas **FeL1**–$A\beta_{1-16}$ shows, in addition to this signal, also a rhombic spin system consistent with low-spin Fe(III) $S = \frac{1}{2}$ species (Table 1 and Fig. S8†). The latter is similar to the spectrum for **FeL1** in the presence of 20 equiv. of 1-MeIm (Fig. S8†) and to reported EPR data for other 6-coordinate low spin Fe(III) corroles (with CN^- and pyridine as axial ligands).[54] These data are consistent with contributions from both mono- and bis-axial ligated **FeL1** in the EPR experiment, likely due to the increased ligand affinity upon freezing the solutions for EPR analysis. Increased bis-axial ligation to **FeL1** is observed for both 1-MeIm and $A\beta_{1-16}$ in solution at lower temperatures (10 °C) by UV-Vis (Fig. S10†), and freezing a 5-coordinate (OEC)Fe(III)(py) corrole (OEC = trianion of 2,3,7,8,12,13,17,18-octaethylcorrole) in pyridine results in a similar spectral pattern with both intermediate and low spin signals.[42b] Due to the distinct temperature-dependence of signal intensity for the EPR spectra of the Fe species it is not possible to accurately determine their ratios from these experiments.[55]

Incubation of both Cu(II) and **FeL1** with $A\beta_{1-16}$ affords the ternary species **FeL1**–$A\beta_{1-16}$–Cu(II) with an EPR spectrum that is essentially the sum of the components $A\beta_{1-16}$–Cu(II) and **FeL1**–$A\beta_{1-16}$ (Fig. 6). The simulation parameters are detailed in Table 1, with the two Cu(II) species Component I and Component II in a 0.7 : 0.3 ratio. While this differs slightly from the ratio for $A\beta_{1-16}$–Cu(II) alone, the limited resolution of the spectra suggests minimal change to the Cu-site upon binding of **FeL1** to the peptide (*vide infra*). Similarly, the simulation parameters for the Fe species present in **FeL1**–$A\beta_{1-16}$–Cu(II) (Table 1) are identical to **FeL1**–$A\beta_{1-16}$ suggesting that while both Cu(II) and **FeL1** bind to $A\beta_{1-16}$, the binding sites are independent of one another as far as can be determined through the EPR experiments. This is reminiscent of reported EPR analysis of Cu(II) and heme with $A\beta_{1-16}$, which also suggested that while both did bind to the peptide there was no observable interaction between the two metal centres.[17a]

Influence of FeL1 on Aβ aggregation

Gel electrophoresis and western blotting, in combination with Transmission Electron Microscopy (TEM), were used to investigate if binding of **FeL1** to the Aβ peptide would alter the size distribution of Aβ species and the morphology of the resulting aggregates. The longer $A\beta_{1-42}$ peptide was employed for this study, as it is most aggregation prone and neurotoxic.[13b,56] Incubation with low concentrations of **FeL1** (0.1 to 1 equiv., for 24 h) significantly affected the aggregation pattern (Fig. 7A). While the $A\beta_{1-42}$ peptide forms mostly high molecular weight aggregates (lane 1) in the absence of **FeL1**, consistent with previous reports,[19a,24b,57] **FeL1** exhibits a concentration-dependent effect on the aggregation pattern (lanes 2–5). Only low molecular weight species were observed after 24 h with one equiv. of **FeL1** (lane 5). The influence of **FeL1** on $A\beta_{1-42}$ aggregation was further confirmed by TEM (Fig. 7B–D). The TEM image for peptide alone shows long fibrils and large aggregate size, matching previous reports.[24b,57] However, as the

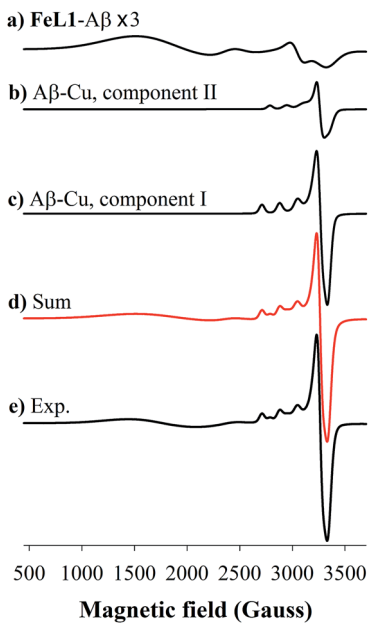

Fig. 6 Frozen-solution EPR spectrum (bottom), corresponding simulation (red) and spectral deconvolution of **FeL1** in the presence of 1 equiv. of both $A\beta_{1-16}$ and Cu(II) at 20 K. (a) **FeL1**–Aβ component simulation (multiplied by a factor of 3), (b) Aβ–Cu(II) Component II simulation (c) Aβ–Cu(II) Component I simulation (d) sum of all simulated species and (e) experimental spectrum. Conditions: $[A\beta_{1-16}] =$ 550 μM, [**FeL1**] = [Cu(II)] = 500 μM, in PBS buffer (0.05 M, pH 7.4). EPR parameters: frequency = 9.38 GHz, microwave power = 2.0 mW, time constant = 40.96 ms, modulation amplitude = 5G, average of five 1 min scans.

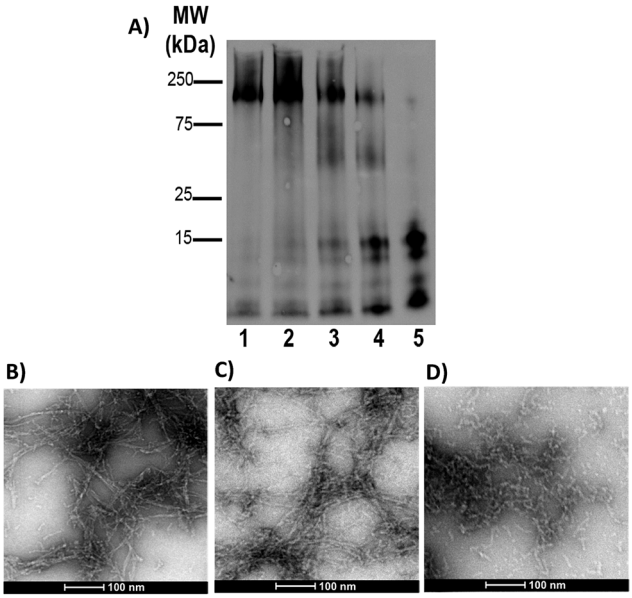

Fig. 7 Influence of **FeL1** on the aggregation profile of $A\beta_{1-42}$. (A) Gel electrophoresis/Western blot of 25 μM $A\beta_{1-42}$ and different concentrations of **FeL1** in PBS buffer (0.01 M, pH 7.4) after 24 h incubation with agitation at 37 °C, using anti-Aβ antibody 6E10. Lane 1: $A\beta_{1-42}$; lane 2: $A\beta_{1-42}$ + **FeL1** (0.1 equiv.); lane 3: $A\beta_{1-42}$ + **FeL1** (0.25 equiv.); lane 4: $A\beta_{1-42}$ + **FeL1** (0.5 equiv.); lane 5: $A\beta_{1-42}$ + **FeL1** (1 equiv.). And TEM images of (B) $A\beta_{1-42}$; (C) $A\beta_{1-42}$ + 0.1 equiv. **FeL1**; and (D) $A\beta_{1-42}$ + 1 eq **FeL1**.

concentration of **FeL1** is increased, a reduction in aggregate size is observed, with only small aggregates present with 1 equiv. of **FeL1** (Fig. 7D). We also investigated the effect of the free ligand **L1** on $A\beta_{1-42}$ peptide aggregation. Under the same experimental conditions, **L1** also displays a concentration-dependent effect on aggregation (Fig. S11†), however aggregate species are observed over a broad molecular weight range. We hypothesize that **L1** alters the aggregation pattern *via* hydrophobic interactions with the Aβ peptide,[19a,37,58] while the covalent interaction of **FeL1** with Aβ His residues results in the preferential formation of low molecular weight species (Fig. 7).

Catalytic antioxidant activity

FeL1 has been previously reported to exhibit exceptional antioxidant activity for the disproportionation of H_2O_2,[30d] dismutation of $O_2^{\bullet-}$,[30a] and catalytic activity for the decomposition of peroxynitrite (PN, $ONOO^-$).[32] In addition, the antioxidant activity of **FeL1** is maintained, and even enhanced, when bound to albumin, lipoproteins, or imidazole since this minimizes formation of the less catalytically-active μ-oxo iron(IV) dimer.[30c,30d] This work highlighted that the **FeL1**–Aβ species could act as a potent antioxidant, and possibly minimize ROS generation from Aβ–Cu(II) when both **FeL1** and Cu(II) are bound to the peptide simultaneously.

Catalase activity. The catalase activity of **FeL1** has been demonstrated to exceed that of any other synthetic mimic of the enzyme,[30d,31,59] and its activity increases in the presence of excess imidazole. In order to determine the influence of **FeL1** binding to $A\beta_{1-16}$ on its catalase activity, an "Amplex Red"/H_2O_2 catalase assay was performed. This assay relies on competing with the very fast color producing reaction by adding a complex that catalytically decomposes H_2O_2. A catalase standard curve (Fig. S12A†) was prepared and different concentrations of **FeL1** in the presence and absence of $A\beta_{1-16}$ (Fig. S12B†) were tested to determine their activity. Both **FeL1** and the 1 : 1 **FeL1**–$A\beta_{1-16}$ adduct displayed good catalase activity, with the latter being superior. This shows that His binding of the Aβ peptide to **FeL1** results in an enhancement of catalase activity at all concentrations studied (1–5 μM).

Aβ–Cu(II) ROS production. Under biologically relevant reducing conditions, which are commonly mimicked by reducing agents such as ascorbate (Asc), Aβ–Cu(II) species are known to produce an array of ROS composed of superoxide anion radical, hydrogen peroxide, and hydroxyl radical.[38b,51] There are many protocols for investigating the multiple steps that lead to these damaging species (Scheme 3), of which the first one is the oxidation of Asc by Cu(II). This process was followed by monitoring the time course for disappearance of the Asc absorption band at 265 nm (Fig. 8) in the presence of $CuCl_2$ and **FeL1** only, their binary adducts with $A\beta_{1-16}$, and the ternary adduct formed by combining $A\beta_{1-16}$ with Cu(II) and **FeL1**. Consistent with previous reports,[51] the high rate of Asc consumption in the presence of Cu(II) is diminished when bound to $A\beta_{1-16}$; and consistent with expectations, both **FeL1** and **FeL1**–Aβ did not promote Asc oxidation. The most revealing result is that the ternary **FeL1**–$A\beta_{1-16}$–Cu(II) complex displayed only slightly enhanced Asc oxidation in comparison to $A\beta_{1-16}$–Cu(II) only. Overall, and in accordance with the EPR results that show that **FeL1** does not alter the Cu(II) binding site, this assay suggests that the presence of **FeL1** does not significantly affect the reduction of Aβ–Cu(II) by Asc.

Cu–Aβ species can transform O_2 to H_2O_2 through a series of steps, which can be detected *via* its reaction with Amplex Red, which forms the intensively colored resorufin (Scheme 3).[60] Following this process by monitoring the formation of resorufin (Fig. 9A) revealed that: (a) Cu(II) alone induces the fastest rate of formation of H_2O_2; (b) the binding of Cu(II) to Aβ slows down the process, as reported previously;[61] and (c) the ternary **FeL1**–$A\beta_{1-16}$–Cu(II) species shows a reduced rate of H_2O_2 formation

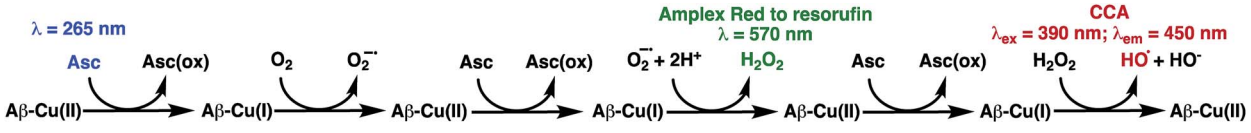

Scheme 3 Reactive oxygen species generated by Aβ–Cu(II) in the presence of ascorbate and the possible assays to detect them, modified from C. Cheignon *et al.* 2018.[38b]

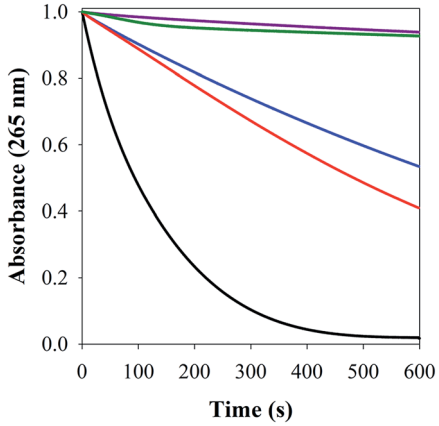

Fig. 8 Ascorbate consumption by Cu(II) (black), Aβ–Cu(II) (blue); **FeL1**–Aβ–Cu(II) (red); **FeL1**–Aβ (purple); **FeL1** (green), measured using UV-Vis spectroscopy ($\lambda = 265$ nm) as a function of time in PBS buffer (0.01 M, pH 7.4). [Asc] = 100 μM, [$A\beta_{1-16}$] = [**FeL1**] = 10 μM and [$CuCl_2$] = 9 μM.

and lower amount overall. The latter phenomenon is consistent with **FeL1** quenching the H_2O_2 that is produced by the bound Cu(II), due to the good catalase-like activity of **FeL1** in both its free form and when bound to the Aβ peptide (Fig. S12B†). In addition to catalase activity, **FeL1** displays exceptional antioxidant activity for the dismutation of $O_2^{\bullet -}$,[30a] and thus the complex may also quench superoxide formed as shown in Scheme 3. Detection of this reactivity using a cytochrome c assay[9b,17b] was challenging due to interference of **FeL1** absorption bands.

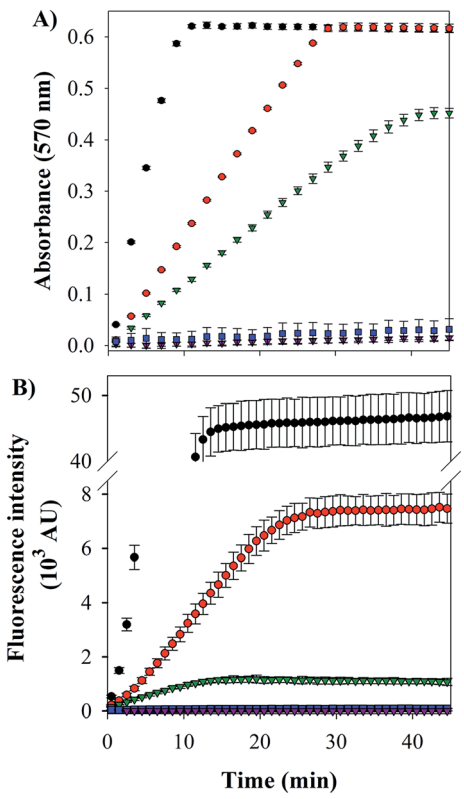

Fig. 9 ROS production by Aβ–Cu(II) in the presence of ascorbate. (A) Amplex red assay for H_2O_2 formation by UV-Vis absorbance at 570 nm. [Asc] = 400 μM, [$A\beta_{1-16}$] = [**FeL1**] = [Cu(II)] = 20 μM, [Amplex red] = 100 μM; [HRP] = 0.4 U mL^{-1} (where 1 unit is defined as the amount of enzyme that will form 1.0 mg purpurogallin from pyrogallol in 20 seconds at pH 6.0 at 20 °C). (B) CCA assay for ·OH formation measured by fluorescence, λ_{ex} 395 nm and λ_{em} 450 nm. [Asc] = 300 μM, [$A\beta_{1-16}$] = [**FeL1**] = [Cu(II)] = 40 μM, [CCA] = 100 μM. ● Cu(II); ● Aβ–Cu(II); ▼ **FeL1**–Aβ–Cu(II); ▼ **FeL1**–Aβ; ■ **FeL1**.

The last and most damaging step in Scheme 3 occurs *via* the formation of the hydroxyl radical (·OH) from the reaction of Cu(I) with H_2O_2 (Scheme 3), which may be detected by the reaction of 3-coumarin carboxylic acid (3-CCA) with ·OH to form the fluorescent 7-hydroxy-3-coumarin-carboxylic acid (7-OH-3-CCA).[62] Consistent with previous reports,[12e] ·OH production is quite fast and significant for Aβ–Cu(II) albeit much less than for non-His-coordinated Cu(II) (Fig. 9B). The addition of **FeL1**, to form the ternary **FeL1**–$A\beta_{1-16}$–Cu(II) species, resulted in a further 6-fold reduction in the amount of 7-OH-3-CCA. In principle, this may reflect either the lower availability of H_2O_2 due to the catalase-like activity or the direct quenching of ·OH by **FeL1**, or a combination of both. Another possible interpretation is that Cu in the ternary complex is less reactive, which is unlikely considering the minimal interaction of **FeL1** with $A\beta_{1-16}$–Cu(II) binding motif. In any case, the almost complete elimination of hydroxyl radical formation demonstrates that the potent antioxidant activity of **FeL1** is maintained when bound to the Aβ peptide.

Summary

This study underlines the ability of **FeL1** to target both Aβ peptide aggregation and ROS formation, two factors influencing AD progression. **FeL1** and the free corrole ligand **L1** influence Aβ aggregation differently; **FeL1** stabilizes low molecular weight species while **L1** stabilizes aggregates over a broad MW range. **FeL1** forms a 1 : 1 adduct with Aβ *via* axial binding of one His residue with a moderate binding affinity (K_d of $\sim 10^{-7}$ M), which is weaker in comparison to Cu binding to Aβ (K_d of $\sim 10^{-10}$ M) but still stronger than Zn(II) binding (K_d of $\sim 10^{-5}$ M).[10b,14a,38a,51] It is interesting to note that **FeL1** has a much higher affinity for Aβ peptide His residues than 1-MeIm or free His, suggesting significant non-covalent interactions between **FeL1** and the Aβ peptide. These results are in agreement with the specific binding of **FeL1** to HDL2 proteins in comparison to other serum constituents, due to the amphipolar character of **FeL1**.[30c] Indeed, **L1** was also shown to influence Aβ peptide aggregation likely due to hydrophobic interactions, albeit to a significantly lower extent. In a similar manner, non-covalent π–π stacking interactions, in addition to covalent binding, have been shown to dictate the association of Pt(II)(phenanthroline) complexes with the Aβ peptide.[21a,29,63]

We have also shown herein that **FeL1** binds to the Aβ peptide concurrently with Cu(II). Our EPR data suggests no significant change in the Cu-binding site with **FeL1** His coordination. This is further corroborated by the ascorbate oxidation assay, which displays only minor changes to the rate of ascorbate oxidation for Aβ–Cu(II) and the ternary species **FeL1**–Aβ–Cu(II). However, the bound **FeL1** acts as an efficient catalase, and decomposes

a significant fraction of the H_2O_2 generated by Aβ–Cu(II) (Fig. 9A). In the presence of **FeL1** we also observe a decrease in the formation of ·OH (Fig. 9B), consistent with the result from the amplex red assay. Our results show that amphipolar **FeL1** binds specifically to the Aβ peptide *via* a His residue in a 1 : 1 stoichiometry, and this interaction modulates the peptide aggregation pathway. In addition, the peptide-bound **FeL1** maintains its exceptional antioxidant activity, limiting ROS formation from Aβ–Cu(II). Overall, our results highlight the promising multifunctional character of **FeL1** to limit Aβ peptide aggregation and the formation of damaging ROS, two hallmarks of AD.

Conflicts of interest

There are no conflicts to declare.

Acknowledgements

This work was supported by Natural Sciences and Engineering Research Council (NSERC) Discovery Grant (T. S., M. A. S., and C. J. W.), a Michael Smith Career Investigator Award (T. S.), and a New Investigator Grant from the Alzheimer's Association (NIRG-15-362537), Brain Canada (to T. S.) and Science without borders (CAPES – Proc. no. 0711/13-6, Brazil to L. M. F. G.). Dr Andrew Lewis is thanked for assistance with NMR measurements. K. E. P. acknowledges a NSERC Vanier CGS for support. Z. G. and A. M. acknowledge The Israel Science Foundation for support.

Notes and references

1 A. W. Martin Prince, M. Guerchet, G.-C. Ali, Yu-T. Wu and M. Prina, *World Alzheimer Report 2015, The Global Impact on Dementia. An Analysis of Prevalence, Incidence, Cost and Trends*, 2015.

2 Dementia statistics, http://www.alz.co.uk/research/statistics, accessed May 24th.

3 (*a*) V. H. Finder, *J. Alzheimer's Dis.*, 2010, **22**, S5–S19; (*b*) E. D. Roberson and L. Mucke, *Science*, 2006, **314**, 781–784; (*c*) P. A. Adlard, S. A. James, A. I. Bush and C. L. Masters, *Drugs Today*, 2009, **45**, 293–304; (*d*) M. Citron, *Nat. Rev. Drug Discovery*, 2010, **9**, 387–398; (*e*) D. J. Selkoe, *Nat. Med.*, 2011, **17**, 1693.

4 J. L. Hickey and P. S. Donnelly, *Coord. Chem. Rev.*, 2012, **256**, 2367–2380.

5 H. W. Querfurth and F. M. LaFerla, *N. Engl. J. Med.*, 2010, **362**, 329–344.

6 M. P. Mazanetz and P. M. Fischer, *Nat. Rev. Drug Discovery*, 2007, **6**, 464–479.

7 (*a*) G. K. W. Kong, J. J. Adams, H. H. Harris, J. F. Boas, C. C. Curtain, D. Galatis, C. L. Masters, K. J. Barnham, W. J. McKinstry, R. Cappai and M. W. Parker, *J. Mol. Biol.*, 2007, **367**, 148–161; (*b*) D. J. Selkoe and D. Schenk, *Annu. Rev. Pharmacol. Toxicol.*, 2003, **43**, 545–584.

8 C. A. McLean, R. A. Cherny, F. W. Fraser, S. J. Fuller, M. J. Smith, K. Beyreuther, A. I. Bush and C. L. Masters, *Ann. Neurol.*, 1999, **46**, 860–866.

9 (*a*) C. L. Masters, G. Simms, N. A. Weinman, G. Multhaup, B. L. McDonald and K. Beyreuther, *Proc. Natl. Acad. Sci. U. S. A.*, 1985, **82**, 4245–4249; (*b*) M. Mital, E. Wezynfeld Nina, T. Frączyk, Z. Wiloch Magdalena, E. Wawrzyniak Urszula, A. Bonna, C. Tumpach, J. Barnham Kevin, L. Haigh Cathryn, W. Bal and C. Drew Simon, *Angew. Chem., Int. Ed.*, 2015, **54**, 10460–10464; (*c*) V. Borghesani, B. Alies and C. Hureau, *Eur. J. Inorg. Chem.*, 2018, **2018**, 7–15.

10 (*a*) D. J. Selkoe and J. Hardy, *EMBO Mol. Med.*, 2016, **8**, 595–608; (*b*) M. C. Heffern, P. T. Velasco, L. M. Matosziuk, J. L. Coomes, C. Karras, M. A. Ratner, W. L. Klein, A. L. Eckermann and T. J. Meade, *ChemBioChem*, 2014, **15**, 1584–1589; (*c*) S. Lesne, M. T. Koh, L. Kotilinek, R. Kayed, C. G. Glabe, A. Yang, M. Gallagher and K. H. Ashe, *Nature*, 2006, **440**, 352–357; (*d*) A. D. Watt, V. L. Villemagne and K. J. Barnham, *J. Alzheimer's Dis.*, 2013, **33**(suppl. 1), S283–S293.

11 D. H. Cho, T. Nakamura, J. G. Fang, P. Cieplak, A. Godzik, Z. Gu and S. A. Lipton, *Science*, 2009, **324**, 102–105.

12 (*a*) E. Nam, J. Han, J.-M. Suh, Y. Yi and M. H. Lim, *Curr. Opin. Chem. Biol.*, 2018, **43**, 8–14; (*b*) S. C. Drew and K. J. Barnham, *Acc. Chem. Res.*, 2011, **44**, 1146–1155; (*c*) E. Gaggelli, H. Kozlowski, D. Valensin and G. Valensin, *Chem. Rev.*, 2006, **106**, 1995–2044; (*d*) J. A. Duce and A. I. Bush, *Prog. Neurobiol.*, 2010, **92**, 1–18; (*e*) C. Cheignon, M. Jones, E. Atrian-Blasco, I. Kieffer, P. Faller, F. Collin and C. Hureau, *Chem. Sci.*, 2017, **8**, 5107–5118; (*f*) Y. Yuan, F. Niu, Y. Liu and N. Lu, *Neurol. Sci.*, 2014, **35**, 923–928.

13 (*a*) M. G. Savelieff, S. Lee, Y. Liu and M. H. Lim, *ACS Chem. Biol.*, **8**, 856–865; (*b*) K. P. Kepp, *Chem. Rev.*, 2012, **112**, 5193–5239; (*c*) T. D. Rae, P. J. Schmidt, R. A. Pufahl, V. C. Culotta and T. V. O'Halloran, *Science*, 1999, **284**, 805–808.

14 (*a*) F. Hane and Z. Leonenko, *Biomolecules*, 2014, **4**, 101–116; (*b*) C. C. Curtain, F. Ali, I. Volitakis, R. A. Cherny, R. S. Norton, K. Beyreuther, C. J. Barrow, C. L. Masters, A. I. Bush and K. J. Barnham, *J. Biol. Chem.*, 2001, **276**, 20466–20473; (*c*) R. J. Ward, D. T. Dexter and R. R. Crichton, *J. Trace Elem. Med. Biol.*, 2015, **31**, 267–273.

15 (*a*) M. A. Lovell, J. D. Robertson, W. J. Teesdale, J. L. Campbell and W. R. Markesbery, *J. Neurosci.*, 1998, **158**, 47–52; (*b*) L. M. Miller, Q. Wang, T. P. Telivala, R. J. Smith, A. Lanzirotti and J. Miklossy, *J. Struct. Biol.*, 2006, **155**, 30–37; (*c*) R. Squitti, *Front. Biosci.*, 2012, **17**, 451–472; (*d*) A. S. Pithadia and M. H. Lim, *Curr. Opin. Chem. Biol.*, 2012, 67–73; (*e*) P. Faller and C. Hureau, *Dalton Trans.*, 2009, 1080–1094, DOI: 10.1039/b813398k.

16 (*a*) A. Lakatos, B. Gyurcsik, N. V. Nagy, Z. Csendes, E. Weber, L. Fulop and T. Kiss, *Dalton Trans.*, 2012, **41**, 1713–1726; (*b*) S. L. Leong, T. R. Young, K. J. Barnham, A. G. Wedd, M. G. Hinds, Z. Xiao and R. Cappai, *Metallomics*, 2014, **6**, 105–116; (*c*) A. S. Pithadia, A. Kochi, M. T. Soper, M. W. Beck, Y. Z. Liu, S. Lee, A. S. DeToma, B. T. Ruotolo and M. H. Lim, *Inorg. Chem.*, 2012, **51**, 12959–12967; (*d*)

F. Bousejra-ElGarah, C. Bijani, Y. Coppel, P. Faller and C. Hureau, *Inorg. Chem.*, 2011, **50**, 9024–9030.

17 (*a*) D. Pramanik, C. Ghosh and S. G. Dey, *J. Am. Chem. Soc.*, 2011, **133**, 15545–15552; (*b*) K. Reybier, S. Ayala, B. Alies, J. V. Rodrigues, S. B. Rodriguez, G. L. Penna, F. Collin, C. M. Gomes, C. Hureau and P. Faller, *Angew. Chem., Int. Ed.*, 2016, **55**, 1085–1089; (*c*) X. Huang, M. P. Cuajungco, C. S. Atwood, M. A. Hartshorn, J. D. A. Tyndall, G. R. Hanson, K. C. Stokes, M. Leopold, G. Multhaup, L. E. Goldstein, R. C. Scarpa, A. J. Saunders, J. Lim, R. D. Moir, C. Glahe, E. F. Bowden, C. L. Masters, D. P. Fairlie, R. E. Tanzi and A. I. Bush, *J. Biol. Chem.*, 1999, **274**, 37111–37116; (*d*) G. F. Z. da Silva and L. J. Ming, *Angew. Chem., Int. Ed.*, 2005, **44**, 5501–5504; (*e*) X. Huang, C. S. Atwood, M. A. Hartshorn, G. Multhaup, L. E. Goldstein, R. C. Scarpa, M. P. Cuajungco, D. N. Gray, J. Lim, R. D. Moir, R. E. Tanzi and A. I. Bush, *Biochemistry*, 1999, **38**, 7609–7616; (*f*) C. Cheignon, P. Faller, D. Testemale, C. Hureau and F. Collin, *Metallomics*, 2016, **8**, 1081–1089.

18 (*a*) M. G. Savelieff, A. S. DeToma, J. S. Derrick and M. H. Lim, *Acc. Chem. Res.*, 2014, **47**, 2475–2482; (*b*) M. C. Carreiras, E. Mendes, M. J. Perry, A. P. Francisco and J. Marco-Contelles, *Curr. Top. Med. Chem.*, 2013, **13**, 1745–1770; (*c*) Z. Liu, A. Zhang, H. Sun, Y. Han, L. Kong and X. Wang, *RSC Adv.*, 2017, **7**, 6046–6058.

19 (*a*) L. M. F. Gomes, R. P. Vieira, M. R. Jones, M. C. P. Wang, C. Dyrager, E. M. Souza-Fagundes, J. G. Da Silva, T. Storr and H. Beraldo, *J. Inorg. Biochem.*, 2014, **139**, 106–116; (*b*) L. Hao, Q. Yunwei and W. Xiaohui, *Future Med. Chem.*, 2018, **10**, 679–701; (*c*) M. R. Jones, E. L. Service, J. R. Thompson, M. C. P. Wang, I. J. Kimsey, A. S. DeToma, A. Ramamoorthy, M. H. Lim and T. Storr, *Metallomics*, 2012, **4**, 910–920; (*d*) X. Wang, X. Wang and Z. Guo, *Coord. Chem. Rev.*, 2018, **362**, 72–84; (*e*) S. Lee, X. Zheng, J. Krishnamoorthy, M. G. Savelieff, H. M. Park, J. R. Brender, J. H. Kim, J. S. Derrick, A. Kochi, H. J. Lee, C. Kim, A. Ramamoorthy, M. T. Bowers and M. H. Lim, *J. Am. Chem. Soc.*, 2014, **136**, 299–310.

20 (*a*) J. J. Miller, L. M. F. Gomes, T. Storr and A. Casini, The Interaction of Metal Compounds with Protein Targets: New Tools in Medicinal Chemistry and Chemical Biology, in *Encyclopedia of Inorganic and Bioinorganic Chemistry*, John Wiley & Sons, Ltd, 2017, DOI: 10.1002/9781119951438.eibc2499; (*b*) K. Chen and M. Cui, *MedChemComm*, 2017, **8**, 1393–1407; (*c*) D. J. Hayne, S. Lim and P. S. Donnelly, *Chem. Soc. Rev.*, 2014, **43**, 6701–6715.

21 (*a*) K. J. Barnham, V. B. Kenche, G. D. Ciccotosto, D. P. Smith, D. J. Tew, X. Liu, K. Perez, G. A. Cranston, T. J. Johanssen, I. Volitakis, A. I. Bush, C. L. Masters, A. R. White, J. P. Smith, R. A. Cherny and R. Cappai, *Proc. Natl. Acad. Sci. U. S. A.*, 2008, **105**, 6813–6818; (*b*) I. Sasaki, C. Bijani, S. Ladeira, V. Bourdon, P. Faller and C. Hureau, *Dalton Trans.*, 2012, **41**, 6404–6407; (*c*) V. A. Streltsov, V. Chandana Epa, S. A. James, Q. I. Churches, J. M. Caine, V. B. Kenche and K. J. Barnham, *Chem. Commun.*, 2013, **49**, 11364–11366; (*d*) F. Collin, I. Sasaki, H. Eury, P. Faller and C. Hureau, *Chem. Commun.*, 2013, **49**, 2130–2132.

22 (*a*) M. R. Jones, C. Mu, M. C. P. Wang, M. I. Webb, C. J. Walsby and T. Storr, *Metallomics*, 2015, **7**, 129–135; (*b*) L. Messori, M. Camarri, T. Ferraro, C. Gabbiani and D. Franceschini, *ACS Med. Chem. Lett.*, 2013, **4**, 329–332.

23 (*a*) G. S. Yellol, J. G. Yellol, V. B. Kenche, X. M. Liu, K. J. Barnham, A. Donaire, C. Janiak and J. Ruiz, *Inorg. Chem.*, 2015, **54**, 470–475; (*b*) L. Lu, H.-J. Zhong, M. Wang, S.-L. Ho, H.-W. Li, C.-H. Leung and D.-L. Ma, *Sci. Rep.*, 2015, **5**, 14619.

24 (*a*) J. Suh, S. H. Yoo, M. G. Kim, K. Jeong, J. Y. Ahn, M.-s. Kim, P. S. Chae, T. Y. Lee, J. Lee, J. Lee, Y. A. Jang and E. H. Ko, *Angew. Chem., Int. Ed.*, 2007, **46**, 7064–7067; (*b*) J. S. Derrick, J. Lee, S. J. C. Lee, Y. Kim, E. Nam, H. Tak, J. Kang, M. Lee, S. H. Kim, K. Park, J. Cho and M. H. Lim, *J. Am. Chem. Soc.*, 2017, **139**, 2234–2244.

25 C. Y. Chan, A. Noor, C. A. McLean, P. S. Donnelly and P. J. Barnard, *Chem. Commun.*, 2017, **53**, 2311–2314.

26 B. Y.-W. Man, H.-M. Chan, C.-H. Leung, D. S.-H. Chan, L.-P. Bai, Z.-H. Jiang, H.-W. Li and D.-L. Ma, *Chem. Sci.*, 2011, **2**, 917–921.

27 (*a*) C. D. Amandine, A. Vinita, G. Régis, D. Nicolas, P. Clotilde and H. Christelle, *Chem.–Eur. J.*, 2018, **24**, 5095–5099; (*b*) R. Walke Gulshan, S. Ranade Dnyanesh, M. Bapat Archika, R. Srikanth and P. Kulkarni Prasad, *ChemistrySelect*, 2016, **1**, 3497–3501.

28 L. He, X. Wang, D. Zhu, C. Zhao and W. Du, *Metallomics*, 2015, **7**, 1562–1572.

29 V. B. Kenche, L. W. Hung, K. Perez, I. Volitakes, G. Ciccotosto, J. Kwok, N. Critch, N. Sherratt, M. Cortes, V. Lal, C. L. Masters, K. Murakami, R. Cappai, P. A. Adlard and K. J. Barnham, *Angew. Chem., Int. Ed.*, 2013, **52**, 3374–3378.

30 (*a*) M. Eckshtain, I. Zilbermann, A. Mahammed, I. Saltsman, Z. Okun, E. Maimon, H. Cohen, D. Meyerstein and Z. Gross, *Dalton Trans.*, 2009, 7879–7882, DOI: 10.1039/b911278b; (*b*) Z. Gross, G. Golubkov and L. Simkhovich, *Angew. Chem., Int. Ed.*, 2000, 4045–4047; (*c*) A. Haber, M. Aviram and Z. Gross, *Chem. Sci.*, 2011, **2**, 295–302; (*d*) A. Mahammed and Z. Gross, *Chem. Commun.*, 2010, **46**, 7040–7042; (*e*) Z. Okun and Z. Gross, *Inorg. Chem.*, 2012, **51**, 8083–8090.

31 A. Mahammed and Z. Gross, *J. Am. Chem. Soc.*, 2005, **127**, 2883–2887.

32 A. Mahammed and Z. Gross, *Angew. Chem., Int. Ed.*, 2006, **45**, 6544–6547.

33 A. Haber, A. Mahammed, B. Fuhrman, N. Volkova, R. Coleman, T. Hayek, M. Aviram and Z. Gross, *Angew. Chem., Int. Ed.*, 2008, **47**, 7896–7900.

34 (*a*) C. Ghosh, M. Seal, S. Mukherjee and S. Ghosh Dey, *Acc. Chem. Res.*, 2015, **48**, 2556–2564; (*b*) M. Seal, S. Mukherjee and S. G. Dey, *Metallomics*, 2016, **8**, 1266–1272; (*c*) S. Mukherjee, M. Seal and S. G. Dey, *J. Biol. Inorg Chem.*, 2014, **19**, 1355–1365.

35 A. Haber, M. Aviram and Z. Gross, *Inorg. Chem.*, 2012, **51**, 28–30.

36 P. Lim, A. Mahammed, Z. Okun, I. Saltsman, Z. Gross, H. B. Gray and J. Termini, *Chem. Res. Toxicol.*, 2012, **25**, 400–409.

37 A. Mahammed, H. B. Gray, J. J. Weaver, K. Sorasaenee and Z. Gross, *Bioconjugate Chem.*, 2004, **15**, 738–746.
38 (*a*) L. Q. Hatcher, L. Hong, W. D. Bush, T. Carducci and J. D. Simon, *J. Phys. Chem. B*, 2008, **112**, 8160–8164; (*b*) C. Cheignon, M. Tomas, D. Bonnefont-Rousselot, P. Faller, C. Hureau and F. Collin, *Redox Biol.*, 2018, **14**, 450–464; (*c*) B. Alies, A. Conte-Daban, S. Sayen, F. Collin, I. Kieffer, E. Guillon, P. Faller and C. Hureau, *Inorg. Chem.*, 2016, **55**, 10499–10509; (*d*) I. Zawisza, M. Rózga and W. Bal, *Coord. Chem. Rev.*, 2012, **256**, 2297–2307.
39 D. Valensin, P. Anzini, E. Gaggelli, N. Gaggelli, G. Tamasi, R. Cini, C. Gabbiani, E. Michelucci, L. Messori, H. Kozlowski and G. Valensin, *Inorg. Chem.*, 2010, **49**, 4720–4722.
40 (*a*) Y. Miller, B. Ma and R. Nussinov, *Coord. Chem. Rev.*, 2012, **256**, 2245–2252; (*b*) V. Wineman-Fisher, D. N. Bloch and Y. Miller, *Coord. Chem. Rev.*, 2016, **327–328**, 20–26; (*c*) S. Parthasarathy, F. Long, Y. Miller, Y. Xiao, D. McElheny, K. Thurber, B. Ma, R. Nussinov and Y. Ishii, *J. Am. Chem. Soc.*, 2011, **133**, 3390–3400; (*d*) Y. Miller, B. Ma and R. Nussinov, *Proc. Natl. Acad. Sci. U. S. A.*, 2010, **107**, 9490–9495.
41 L. Alderighi, P. Gans, A. Ienco, D. Peters, A. Sabatini and A. Vacca, *Coord. Chem. Rev.*, 1999, **184**, 311–318.
42 (*a*) C. A. Joseph and P. C. Ford, *J. Am. Chem. Soc.*, 2005, **127**, 6737–6743; (*b*) E. Van Caemelbecke, S. Will, M. Autret, V. A. Adamian, J. Lex, J.-P. Gisselbrecht, M. Gross, E. Vogel and K. M. Kadish, *Inorg. Chem.*, 1996, **35**, 184–192; (*c*) E. Vogel, S. Will, A. S. Tilling, L. Neumann, J. Lex, E. Bill, A. X. Trautwein and K. Wieghardt, *Angew. Chem., Int. Ed.*, 1994, **33**, 731–735.
43 F. A. Walker, M.-W. Lo and M. T. Ree, *J. Am. Chem. Soc.*, 1976, **98**, 5552–5560.
44 D. Sellmann, S. Emig and F. W. Heinemann, *Angew. Chem., Int. Ed.*, 1997, **36**, 1734–1736.
45 P. Gans, A. Sabatini and A. Vacca, *Ann. Chim.*, 1999, **89**, 45–49.
46 T. Kowalik-Jankowska, M. Ruta, K. Wiśniewska and L. Łankiewicz, *J. Inorg. Biochem.*, 2003, **95**, 270–282.
47 (*a*) A. E. Martell and R. D. Hancock, *Metal Complexes in Aqueous Solutions*, Plenum Press, New York, 1996; (*b*) J.-S. Choi, J. J. Braymer, R. P. R. Nanga, A. Ramamoorthy and M. H. Lim, *Proc. Natl. Acad. Sci. U. S. A.*, 2010, **107**, 21990–21995; (*c*) W. R. Harris, C. J. Carrano and K. N. Raymond, *J. Am. Chem. Soc.*, 1979, **101**, 2722–2727.
48 Z. Xiao and A. G. Wedd, *Nat. Prod. Rep.*, 2010, **27**, 768–789.
49 T. S. Choi, H. J. Lee, J. Y. Han, M. H. Lim and H. I. Kim, *J. Am. Chem. Soc.*, 2017, **139**, 15437–15445.
50 H. Eury, C. Bijani, P. Faller and C. Hureau, *Angew. Chem., Int. Ed. Engl.*, 2011, **50**, 901–905.
51 E. Atrián-Blasco, M. del Barrio, P. Faller and C. Hureau, *Anal. Chem.*, 2018, **90**, 5909–5915.
52 (*a*) B. Alies, I. Sasaki, O. Proux, S. Sayen, E. Guillon, P. Faller and C. Hureau, *Chem. Commun.*, 2013, **49**, 1214–1216; (*b*) S. C. Drew, C. J. Noble, C. L. Masters, G. R. Hanson and K. J. Barnham, *J. Am. Chem. Soc.*, 2009, **131**, 1195–1207; (*c*) C. Hureau and P. Dorlet, *Coord. Chem. Rev.*, 2012, **256**, 2175–2187.
53 G. Palmer, *Iron Porphyrins. Part II*, Addison-Wesley Publ. Co., Reading, MA, 1983.
54 (*a*) S. Cai, S. Licoccia and F. A. Walker, *Inorg. Chem.*, 2001, **40**, 5795–5798; (*b*) L. Simkhovich, I. Goldberg and Z. Gross, *Inorg. Chem.*, 2002, **41**, 5433–5439.
55 L. V. Liu, S. Hong, J. Cho, W. Nam and E. I. Solomon, *J. Am. Chem. Soc.*, 2013, **135**, 3286–3299.
56 (*a*) D. M. Walsh and D. J. Selkoe, *J. Neurochem.*, 2007, **101**, 1172–1184; (*b*) C. Haass and D. J. Selkoe, *Nat. Rev. Mol. Cell Biol.*, 2007, **8**, 101–112; (*c*) Y. S. Gong, L. Chang, K. L. Viola, P. N. Lacor, M. P. Lambert, C. E. Finch, G. A. Krafft and W. L. Klein, *Proc. Natl. Acad. Sci. U. S. A.*, 2003, **100**, 10417–10422; (*d*) R. Jakob-Roetne and H. Jacobsen, *Angew. Chem., Int. Ed.*, 2009, **48**, 3030–3059.
57 M. R. Jones, E. Mathieu, C. Dyrager, S. Faissner, Z. Vaillancourt, K. J. Korshavn, M. H. Lim, A. Ramamoorthy, V. Wee Yong, S. Tsutsui, P. K. Stys and T. Storr, *Chem. Sci.*, 2017, **8**, 5636–5643.
58 (*a*) H. Kroth, A. Ansaloni, Y. Varisco, A. Jan, N. Sreenivasachary, N. Rezaei-Ghaleh, V. Giriens, S. Lohmann, M. P. Lopez-Deber, O. Adolfsson, M. Pihlgren, P. Paganetti, W. Froestl, L. Nagel-Steger, D. Willbold, T. Schrader, M. Zweckstetter, A. Pfeifer, H. A. Lashuel and A. Muhs, *J. Biol. Chem.*, 2012, **287**, 34786–34800; (*b*) M. G. Savelieff, Y. Liu, R. R. P. Senthamarai, K. J. Korshavn, H. J. Lee, A. Ramamoorthy and M. H. Lim, *Chem. Commun.*, 2014, **50**, 5301–5303.
59 A. Mahammed and Z. Gross, *Catal. Sci. Technol.*, 2011, **1**, 535–540.
60 M. Zhou, Z. Diwu, N. Panchuk-Voloshina and R. P. Haugland, *Anal. Biochem.*, 1997, **253**, 162–168.
61 S. Chassaing, F. Collin, P. Dorlet, J. Gout, C. Hureau and P. Faller, *Curr. Top. Med. Chem.*, 2012, **12**, 2573–2595.
62 M. Jensen, A. Canning, S. Chiha, P. Bouquerel, J. T. Pedersen, J. Østergaard, O. Cuvillier, I. Sasaki, C. Hureau and P. Faller, *Chem.–Eur. J.*, 2012, **18**, 4836–4839.
63 (*a*) S. G. Yao, R. A. Cherny, A. I. Bush, C. L. Masters and K. J. Barnham, *J. Pept. Sci.*, 2004, **10**, 210–217; (*b*) G. Ma, F. Huang, X. Pu, L. Jia, T. Jiang, L. Li and Y. Liu, *Chem.–Eur. J.*, 2011, **17**, 11657–11666; (*c*) M. Turner, J. A. Platts and R. J. Deeth, *J. Chem. Theory Comput.*, 2016, **12**, 1385–1392.